Preprints.org

Article

Transcriptomic Analysis of CRISPR/Cas9-Mediated TDP1-Knockout HEK293A Cells

Nadezhda S. Dyrkheeva , Alexandra L. Zakharenko , Anastasia A. Malakhova , Larisa S. Okorokova , Dmitry N. Shtokalo , Sergey P. Medvedev , Alexey A. Tupikin , Marsel R. Kabilov , Olga I. Lavrik [*]

Article

Transcriptomic Analysis of CRISPR/Cas9-Mediated TDP1-Knockout HEK293A Cells

**Nadezhda S. Dyrkheeva [1], Alexandra L. Zakharenko [1], Anastasia A. Malakhova [1,2],
Larisa S. Okorokova [3], Dmitry N. Shtokalo [3,4], Sergey P. Medvedev [1,2], Alexey A. Tupikin [1],
Marsel R. Kabilov [1] and Olga I. Lavrik [1,***

[1] Institute of Chemical Biology and Fundamental Medicine, Siberian Branch of the Russian Academy of Sciences, 8 Lavrentyeva Ave., 630090 Novosibirsk, Russia; dyrkheeva.n.s@gmail.com (N.S.D.), a.zakharenko73@gmail.com (A.L.Z.), kabilov@niboch.nsc.ru (M.R.K.), alenare@niboch.nsc.ru (A.A.T.), lavrik@niboch.nsc.ru (O.I.L.)

[2] Federal Research Center Institute of Cytology and Genetics, Siberian Branch of the Russian Academy of Sciences, 10 Lavrentyeva Ave., 630090 Novosibirsk, Russia; amal@bionet.nsc.ru (A.A.M.), medvedev@bionet.nsc.ru (S.P.M.)

[3] AcademGene LLC, 6 Lavrentyeva Ave., 630090 Novosibirsk, Russia; larisaok123@gmail.com (L.S.O.)

[4] A.P. Ershov Institute of Informatics Systems SB RAS, 6 Lavrentyeva Ave., 630090 Novosibirsk, Russia; shtokalod2@gmail.com (D.N.S.)

* Correspondence: Olga I. Lavrik lavrik@niboch.nsc.ru

Abstract: Tyrosyl-DNA phosphodiesterase 1 (TDP1) is a human DNA repair protein. It is a member of the phospholipase D family based on the structure similarity. TDP1 is a key enzyme involved in repairing stalled topoisomerase 1 (TOP1)-DNA complexes. Previously we obtained with the CRISPR/Cas9 method HEK293A cells with the homozygous knockout of the Tdp1 gene and used knockout cells as a cellular model for studying the mechanisms of anticancer therapy. In this work we studied for the first time by transcriptomic analysis the effect of Tdp1 gene knockout on genes expression changes in human HEK293A cell line. We received original data that may indicate a role of TDP1 in other process besides repair of DNA-TOP1 complex. The differentially expressed genes (DEGs) analysis revealed that TDP1 could be involved in different processes such as cell adhesion and communication, spermatogenesis, mitochondrial function, neurodegeneration, cytokine response, and MAPK pathway signaling.

Keywords: tyrosyl-DNA phosphodiesterase 1; topoisomerase 1; HEK293A; transcriptome; TDP1 knockout

1. Introduction

Tyrosyl-DNA phosphodiesterase 1 (TDP1) is a human protein that is encoded by the TDP1 gene [1]. TDP1 is a member of the phospholipase D family based on the structure similarity. It is a key enzyme that is involved in repairing stalled topoisomerase 1 (TOP1)-DNA complexes [2,3]. TOP1 controls the DNA topology removing supercoils during transcription and replication by cutting one of two DNA strands, the strand relaxation, and religation of the strand [4]. TOP1 creates a 3' phosphotyrosyl TOP1-DNA transient intermediate [4] which is normally short-lived, but can be stalled forming the stable TOP1-DNA cleavage complex (TOP1cc). TDP1 catalyzes the hydrolysis of the phosphodiester bond between the tyrosine residue of TOP1 and the 3'-DNA phosphate in TOP1-cc [2]. Mutations in Tdp1 gene are associated with the disease Spinocerebellar Ataxia with Axonal Neuropathy Type 1 (SCAN1) [5]. TDP1 may also remove 3'-glycolate, other modified products and DNA covalent adducts of various origins, for example 3'-blocking residues derived from incorporation of chain terminating antiviral or anticancer nucleosides from 3'-end of single-stranded DNA [6]. TDP1 also has AP-hydrolyzing [7] and transphosphooligonucleotidation activities [8]. It was shown that TDP1 is required for efficient non-homologous end joining in human cells [9]. It is

known that TDP1 promotes oxidative phosphorylation and it is able to act not only in nucleoplasm, but also on mitochondrial protein-linked DNA breaks [10]. It was shown that TDP1 binds PARP1, and the PARylation recruits TDP1 to DNA damage sites without inactivation, stabilizing TDP1 [11]. In addition to PARylation, TDP1 was shown to be phosphorylated by DNA-PK and ATM and SUMOylated in response to transcription-associated TOP1ccs in neurons [12–14]. Different authors highlight the significance of the step catalyzed by TDP1 in neurodegeneration and also in cancer development due to the induction of DNA breaks during anticancer chemotherapy and radiotherapy [10,15–18].

TDP1 has altered expression level in different cancers, both decreased and increased [19–21]. For example, TDP1 deficiency was discovered in two human lung cancer cell lines of the 60 cell lines of the NCI-60 [22]. Overexpression of TDP1 in rhabdomyosarcoma [21] and other cancers could lead to failure in the clinical trial with TOP1 poison irinotecan or topotecan. It is known that TDP1 could be one of the factors of resistance of tumor cells to these anticancer drugs in cancers with increased level of this enzyme because TDP1 prevents the action of topotecan by hydrolyzing TOP1cc-topotecan complex [19,23,24]. It was shown that the inhibition of TDP1 can restore sensitivity to topotecan [25]. In our works we have demonstrated that the TDP1 inhibitor adding in combination with topotecan reveals to synergistic effect both in vitro and in vivo [3,17]. Thus TDP1 is regarded as a potential therapeutic target in cancer therapy.

In this work, we studied for the first time the effect of Tdp1 gene knockout on genes expression changes by transcriptomic analysis in human cell line HEK293A. The novelty of our work lies in the characterization of TDP1 as a participant of different cell processes, not only in DNA repair and in an ensemble with topoisomerases. The differentially expressed genes (DEGs) analysis revealed that TDP1 is important in different processes such as spermatogenesis, cell adhesion and communication, mitochondrial work, neurodegeneration, MAPK pathway signaling.

2. Results

2.1. TDP1 knockout samples preparation

Previously we described obtaining of HEK293A cell line with the homozygous knockout of the Tdp1 gene with the CRISPR/Cas9 method [26]. The scheme of deletion in Tdp1 gene is shown on (Figure S1A). We demonstrated that there was no 3′-phosphotyrosyl TDP1 cleavage activity in the cell extracts of TDP1-knockout (TDP1-KO) cells (C6, G6, F7) in contrast to control HEK293A wild-type (WT) cells and purified TDP1 [26]. We also confirmed the depletion of TDP1 in TDP1-KO cells by western-blot analysis (Figure S1B).

TDP1 knockout markedly changed HEK293A cells morphology of all three TDP1-KO cell clones C6, G6, F7 (Figure S1C). Wild type cells tend to unite into colonies with tighter intercellular contacts than knockout cells. The shapes of the mutant cells are more flat, they more spread out with a low planting density, cells often lie separately, at a distance from each other nearly the same for all three clones.

For these samples we studied for the first time the effect of Tdp1 gene knockout on transcriptome of HEK293A cells by RNA isolation, and next RNA-seq analysis. The RNA samples for the gene expression studies were prepared for HEK293A WT and three biological replicates of TDP1-KO HEK293A cell lines: cell clones C6; G6; F7. After sequencing we analyzed the differentially expressed genes (DEGs) for these four samples.

2.2. Real-time detection of cell sensitivity to topotecan for TDP1 knockout samples

Previously we have shown by a colorimetric assay for assessing cell metabolic activity that three obtained TDP1-KO HEK293A cell clones (C6, G6, F7) were more sensitive to topotecan than WT HEK293A cells [26], what is typical for cells with TDP1-KO. The sensitivity of C6, G6, F7 was confirmed in this work by real-time analysis of cell growth with the impedance-based assay on xCelligence Real-Time Cell Analyzer (Agilent) (Figure 1). The slope of the cell index curve (Figure 1A) was calculated in the 2 hours interval after topotecan addition within the next 24 hours. It is

shown on Figure 1B that WT HEK293A cells are not sensitive to 30 (green) and 60 (dark blue) nM topotecan unlike TDP1-KO HEK293A cell clones.
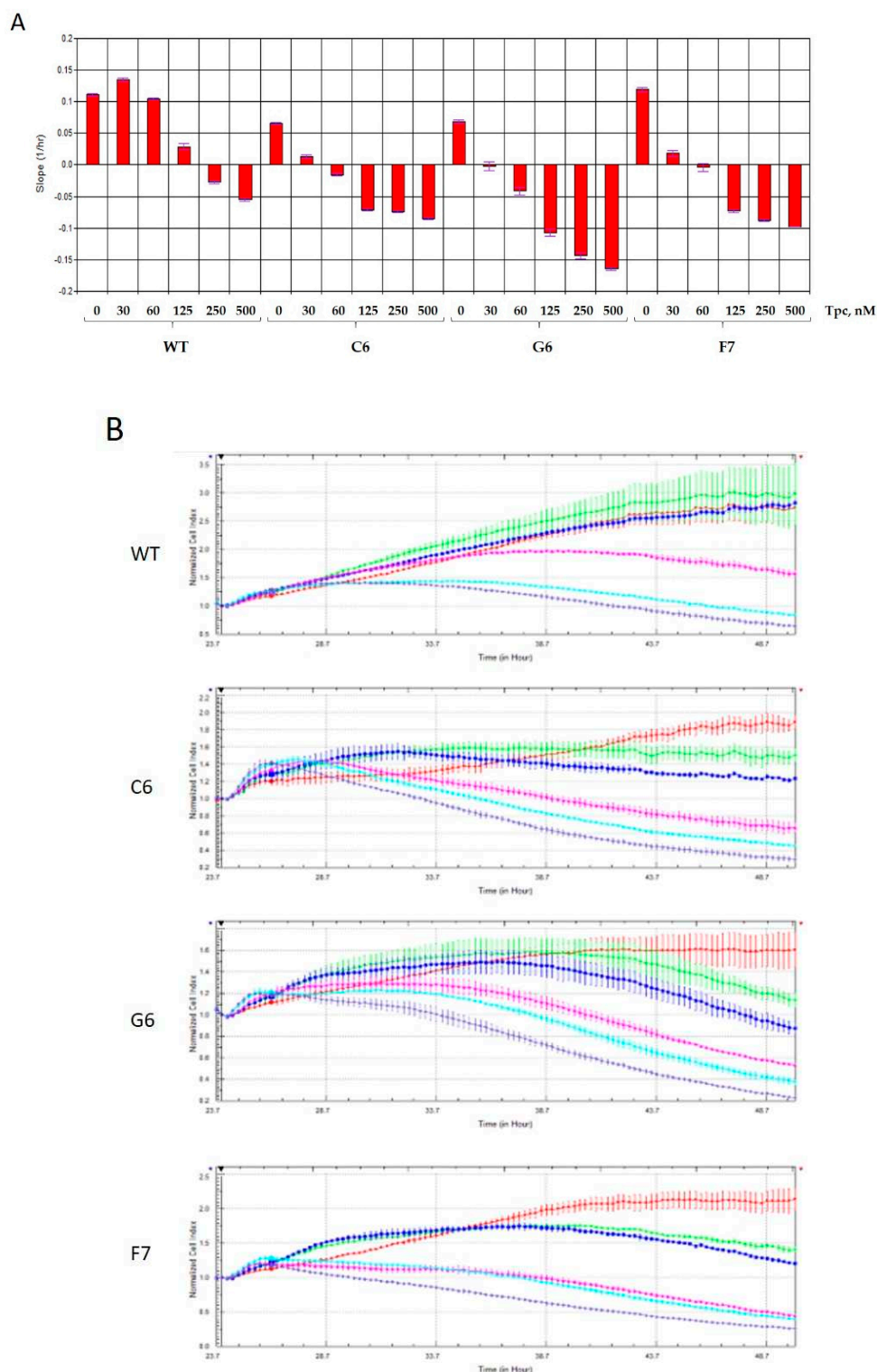
Figure 1. Typical experiment of cell growth of WT HEK293A or TDP1-KO HEK293A cells according to impedance-based real-time assay on xCelligence RTCA (Agilent). Tpc was added to the medium 21 hours after start. A) Slope shows the cell growth speed (1/hr) in the wells without topotecan (Tpc) or with 30, 60, 125, 250, 500 nM Tpc. B) HEK293A WT and TDP1-KO (C6, G6, F7) real-time curves of cells viability. Cell growth in the control wells without Tpc (red), with 30 (green), 60 (blue), 125 (pink), 250 (cyan), 500 (violet) nM topotecan.

2.3. TDP1 knockout effect on transcriptome

We analyzed the effect of TDP1 knockout by bulk transcriptome sequencing of the control HEK293A WT cell line and three TDP1-KO biological replicates: C6, G6, and F7 cell clones, in four technical repeats. Principal component analysis (PCA) was used to determine the data clustering, and it was found that three TDP1-KO cell clones were different on PCA plot (Figure S2). The transcriptional pattern has changed for TDP1-KO HEK293A cells compared to WT cells (Figure 2A, Figure S3). Various changes in cell clones with TDP1-KO affecting transcriptional pattern were identified for cell clones C6, G6, F7 (Figure 2B, Figure S3). We compared gene expression levels after counts quantification and normalization in TDP1-deficient cell lines with a control cell line by estimating values of expression fold change in a logarithmic scale (log2FoldChange) and applying a p-value adjustment procedure. To examine genes under the TDP1 knockout effect that changed their expression on the transcription level, we cut off genes with adjusted p-values under 0.01 and fold change more than 2 (log2FoldChange>1, Figure 2A, Tables 1 and 2).
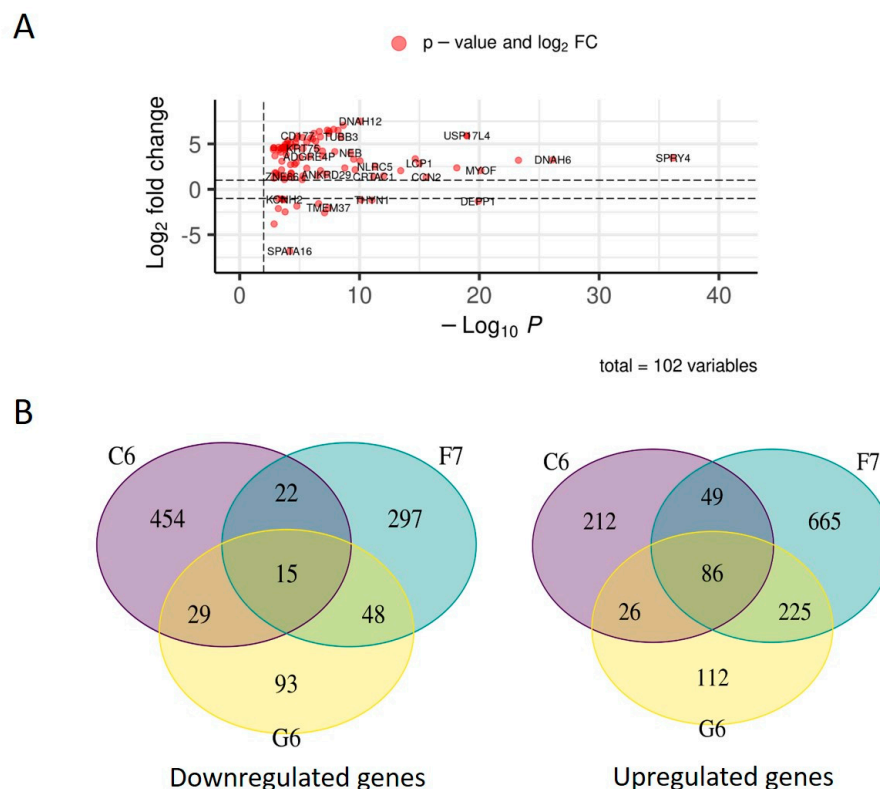

Figure 2. TDP1 knockout effect. A) TDP1-KO cells versus WT HEK293A cells. Volcano Plot for differential gene expression (DEG); B) Venn diagrams of the differentially expressed genes in TDP1-deficient cells compared to the control WT HEK293A cell line.

The number of DEGs for the three cell clones is shown in the barplot/Venn diagram (Figure 2B, Figure S4). Significant differences in differentially expressed genes (DEGs) between cell clones were observed. When comparing WT cells with TDP1-KO cells the less amount of DEGs were found for the G6 cell clone (113 genes were upregulated, and 93 genes were downregulated, Figure S4). Differential gene expression analysis revealed more DEGs for C6 and F7 cells: 458 and 299 downregulated genes, and 215 and 669 upregulated genes, respectively (Figure S4). Thus, the F7 cell clone was found to be most susceptible to TDP1 knockout (Figure 2B).

The number of the DEGs common to all three cell clones C6, G6, and F7 are shown in the barplot/Venn diagram as the intersection (Figure 2B, Figure S4). Thus, TDP1 knockout affected nearly a hundred of common DEGs: 86 genes were upregulated, and 15 genes were downregulated. Most of the DEGs were protein coding. Among the downregulated genes, we identified 9 protein coding and 6 non-coding RNA genes (Table 1). The protein gene SPATA16 (Spermatogenesis Associated 16)

with the highest log2FoldChange value among the downregulated genes (Table 1, highlighted in pink) encodes a testis-specific protein that belongs to the tetratricopeptide repeat-like superfamily and plays a role in spermatogenesis [27]. Another gene DEPP1 (DEPP Autophagy Regulator 1) had a high log2FoldChange value only for the C6 cell clone (Table 1). Other downregulated genes (KCNH2, SYNDIG1, SERPINF1, THYN1, STX8, TMEM37, EMID1) had a log2FoldChange value of about 1-2.

Table 1. Downregulated differentially expressed genes common for three TDP1-KO cell clones (C6, G6, F7).

		log2FoldChange			p-value			p-adj		
		C6	G6	F7	C6	G6	F7	C6	G6	F7
1	KCNH2	-1.357	-1.111	-1.139	1.6e-05	3.2e-04	1.9e-04	2.7e-04	0.004	0.002
2	SYNDIG1	-1.733	-1.12	-1.572	4.5e-08	2.4e-04	2.6e-07	1.9e-06	0.003	6.1e-06
3	SERPINF1	-1.141	-1.698	-1.108	2.2e-04	5.1e-08	2.5e-04	0.002	3.2e-06	0.002
4	SPATA16	-6.098	-5.687	-6.829	3.7e-04	8.6e-04	6.7e-05	0.003	0.008	7.2e-04
5	THYN1	-2.172	-1.045	-1.188	3.8e-30	2.8e-09	9.2e-12	4.2e-27	2.6e-07	5.8e-10
6	DEPP1	-4.185	-1.794	-1.31	1.6e-17	7.0e-37	1.2e-20	3.0e-16	3.5e-33	3.0e-18
7	STX8	-1.104	-1.247	-1.157	1.0e-09	4.0e-12	7.2e-11	7.4e-08	8.4e-10	3.9e-09
8	TMEM37	-1.735	-2.303	-2.042	4.7e-06	1.8e-09	4.0e-08	1.0e-04	1.8e-07	1.2e-06
9	EMID1	-1.112	-1.242	-1.078	2.8e-04	4.3e-05	3.0e-04	0.003	8.4e-04	0.002

Among the upregulated genes, we identified 63 protein coding and 23 protein non-coding DEGs, there were 12 pseudogenes and 11 long non-coding RNA genes (Table 2). Many of the upregulated genes (Table 2) with the high log2FoldChange value (>2 for all three cell clones, highlighted in pink) are involved in different important cell metabolism processes such as transcription, membrane formation, apoptosis, spermatogenesis, protein processing, extracellular matrix organization, and others. The most changed DEG was DNAH12 (Dynein Axonemal Heavy Chain 12) with the highest log2FoldChange value for two cell clones (>6, or more than 64 times for two cell clones). This protein belongs to dyneins family of cytoskeletal motor proteins. The expression level of the other protein gene from this family (DNAH6) was also changed, but not so significantly (Table 2).

Table 2. Upregulated differentially expressed genes common for three TDP1-KO cell clones (C6, G6, F7).

		log2FoldChange			p-value			p-adj		
		C6	G6	F7	C6	G6	F7	C6	G6	F7
1	TAC1	1.248	1.678	2.156	4.2e-04	1.2e-06	2.3e-10	0.004	4.7e-05	1.1e-08

2	ETV1	4.205	2.873	3.36	3.2e-23	2.3e-11	2.2e-15	2.4e-20	4.0e-09	2.6e-13
3	SLAMF7	2.056	2.3	2.145	6.6e-04	1.2e-04	3.2e-04	0.005	0.002	0.003
4	ADAM28	5.679	5.821	6.159	5.3e-07	2.3e-07	3.6e-08	1.6e-05	1.2e-05	1.1e-06
5	PMS2P4	1.786	1.726	1.585	1.6e-04	2.3e-04	6.6e-04	0.002	0.003	0.005
6	LRP2	2.223	1.749	1.807	7.3e-07	1.0e-04	5.1e-05	2.1e-05	0.002	5.7e-04
7	CRTAC1	1.092	1.346	1.373	1.1e-07	2.8e-11	6.7e-12	4.3e-06	4.6e-09	4.3e-10
8	RSPO4	5.947	5.69	6.382	1.8e-06	4.8e-06	2.3e-07	4.6e-05	1.5e-04	5.5e-06
9	CEMIP	2.813	3.226	3.099	0.001	1.8e-04	3.0e-04	0.009	0.003	0.003
10	ELAVL2	5.263	6.616	4.564	1.3e-05	2.9e-08	1.5e-04	2.3e-04	1.9e-06	0.001
11	DNAH6	1.064	1.722	3.259	8.0e-04	2.7e-08	7.3e-27	0.006	1.8e-06	4.2e-24
12	KCNQ4	1.119	1.294	1.524	3.0e-04	2.0e-05	3.1e-07	0.003	4.5e-04	7.2e-06
13	CCN2	1.089	1.108	1.32	1.7e-11	7.2e-12	2.7e-16	2.0e-09	1.4e-09	3.7e-14
14	CFAP58	3.094	2.781	2.92	7.3e-06	5.5e-05	2.0e-05	1.4e-04	0.001	2.6e-04
15	LRRN4	4.372	4.71	4.934	1.0e-03	3.4e-04	1.6e-04	0.007	0.004	0.001
16	HOXD1	3.674	4.914	5.783	0.001	1.1e-05	1.9e-07	0.009	2.8e-04	4.6e-06
17	CHAC1	1.582	1.857	2.057	9.4e-05	3.2e-06	1.8e-07	0.001	1.1e-04	4.4e-06
18	CYP27A1	4.16	4.852	5.142	9.4e-04	7.4e-05	2.2e-05	0.007	0.001	2.8e-04
19	LCP1	1.504	2.367	2.837	6.4e-05	4.7e-11	1.0e-15	8.1e-04	7.1e-09	1.2e-13
20	THBS1	1.198	1.392	1.331	6.9e-04	6.9e-05	1.3e-04	0.005	0.001	0.001
21	MYOF	1.54	1.841	2.07	4.6e-12	9.9e-17	7.4e-21	6.1e-10	5.1e-14	1.9e-18

22	STAT4	3.788	2.958	4.147	2.8e-07	7.2e-05	1.2e-08	9.4e-06	0.001	3.9e-07
23	CYP1A1	1.688	1.873	3.2	3.1e-07	8.2e-09	5.4e-24	1.0e-05	6.5e-07	2.3e-21
24	NLRC5	1.184	1.837	2.477	0.001	3.9e-07	5.1e-12	0.009	1.8e-05	3.4e-10
25	FLG	4.694	5.152	6.603	8.1e-05	1.2e-05	1.4e-08	9.8e-04	3.1e-04	4.7e-07
26	BEND6	2.52	1.596	1.223	2.5e-11	3.0e-05	0.001	2.8e-09	6.2e-04	0.008
27	ANKRD29	2.078	1.018	1.613	3.6e-12	7.9e-04	5.9e-08	4.8e-10	0.008	1.7e-06
28	ADGRG4	7.682	5.224	4.621	6.0e-10	3.5e-05	2.6e-04	4.7e-08	7.1e-04	0.002
29	ZNF66	1.866	1.314	1.413	2.0e-06	8.7e-04	2.9e-04	5.1e-05	0.008	0.002
30	PPP1R32	4.354	4.496	4.625	1.9e-04	1.1e-04	6.1e-05	0.002	0.002	6.6e-04
31	SLC25A34	4.231	4.381	4.656	6.5e-04	3.7e-04	1.3e-04	0.005	0.004	0.001
32	COL6A3	1.836	1.868	3.135	2.1e-04	1.5e-04	9.1e-11	0.002	0.002	4.9e-09
33	DNAJC5G	4.164	4.086	4.386	4.2e-04	5.2e-04	1.7e-04	0.004	0.006	0.002
34	GBX1	4.975	5.374	4.563	3.9e-05	7.4e-06	1.5e-04	5.4e-04	2.1e-04	0.001
35	NOXRED1	4.366	4.502	4.513	6.4e-04	3.9e-04	3.5e-04	0.005	0.005	0.003
36	KRT75	3.589	4.766	4.49	3.7e-04	1.4e-06	5.2e-06	0.003	5.1e-05	8.4e-05
37	NHLH1	4.121	4.537	4.684	2.5e-04	4.5e-05	2.3e-05	0.002	8.6e-04	3.0e-04
38	ABCD2	4.626	4.55	4.623	6.3e-04	7.4e-04	5.7e-04	0.005	0.008	0.004
39	DNAH12	4.865	6.219	7.498	4.7e-05	9.5e-08	8.6e-11	6.4e-04	5.3e-06	4.6e-09
40	CCDC168	4.552	4.418	4.08	7.6e-05	1.2e-04	3.7e-04	9.4e-04	0.002	0.003
41	KLHL11	1.164	1.35	1.29	2.6e-04	2.0e-05	4.3e-05	0.002	4.5e-04	5.0e-04

42	NRIP1	1.391	1.022	1.071	4.8e-09	1.7e-05	6.1e-06	2.8e-07	4.0e-04	9.6e-05
43	ANKRD30B	4.693	5.804	5.366	8.2e-04	2.4e-05	9.5e-05	0.006	5.4e-04	9.7e-04
44	IZUMO1	4.684	4.473	4.33	2.0e-04	3.8e-04	5.5e-04	0.002	0.005	0.004
45	NEB	3.136	2.901	3.996	1.8e-06	9.6e-06	5.5e-10	4.6e-05	2.5e-04	2.5e-08
46	SMG1P5	1.843	2.081	1.824	0.001	2.1e-04	0.001	0.008	0.003	0.007
47	CCR4	5.068	5.669	6.526	3.6e-05	2.7e-06	4.8e-08	5.1e-04	9.2e-05	1.4e-06
48	TMEM232	5.137	5.778	6.399	1.5e-05	7.9e-07	3.5e-08	2.6e-04	3.3e-05	1.0e-06
49	SPRY4	1.947	3.151	3.446	3.7e-12	8.5e-31	6.8e-37	4.9e-10	2.4e-27	6.9e-34
50	SBSN	3.75	4.183	5.544	0.001	2.5e-04	8.4e-07	0.008	0.003	1.7e-05
51	UBE2Q2P1	1.488	1.806	1.73	6.2e-04	2.6e-05	5.1e-05	0.005	5.6e-04	5.7e-04
52	CACNA1E	5.203	5.149	5.616	9.0e-05	1.0e-04	1.8e-05	0.001	0.002	2.4e-04
53	DISP3	2.574	2.956	3.504	0.001	2.1e-04	9.1e-06	0.009	0.003	1.4e-04
54	CD177	4.994	5.479	5.877	3.0e-04	6.0e-05	1.5e-05	0.003	0.001	2.0e-04
55	FRG2	3.419	5.366	5.295	0.002	3.3e-07	4.5e-07	0.01	1.6e-05	1.0e-05
56	ZNF844	2.823	2.47	2.719	3.7e-05	3.1e-04	5.7e-05	5.3e-04	0.004	6.3e-04
57	BAZ2B	6.069	4.744	4.38	9.2e-06	6.1e-04	0.002	1.7e-04	0.007	0.009
58	USP17L4	2.33	4.951	5.903	7.7e-04	3.8e-14	1.1e-19	0.006	1.2e-11	2.5e-17
59	USP17L7	2.33	4.951	5.903	7.7e-04	3.8e-14	1.1e-19	0.006	1.2e-11	2.5e-17
60	SPANXB1	3.724	4.146	5.179	9.9e-04	2.0e-04	2.5e-06	0.007	0.003	4.6e-05
61	ACVR2B-AS1	1.743	2.332	1.776	0.001	1.3e-05	9.4e-04	0.009	3.3e-04	0.006

62	IDI2-AS1	4.245	5.235	5.706	0.001	3.7e-05	5.5e-06	0.008	7.4e-04	8.8e-05
63	KRTAP5-AS1	2.373	2.095	3.317	1.2e-05	1.1e-04	3.1e-10	2.1e-04	0.002	1.5e-08
64	RNF217-AS1	5.109	5.21	4.564	3.7e-04	2.6e-04	0.001	0.003	0.003	0.009
65	SMG1P1	2.219	2.956	2.748	8.5e-04	6.3e-06	2.6e-05	0.006	1.8e-04	3.3e-04
66	ARHGAP31-AS1	4.286	5.36	5.638	3.3e-04	4.5e-06	1.2e-06	0.003	1.4e-04	2.4e-05
67	ETV5	1.784	2.383	2.364	3.2e-11	4.7e-19	7.6e-19	3.4e-09	3.2e-16	1.5e-16
68	TUBB3	3.8	4.068	5.783	1.6e-04	4.4e-05	3.7e-09	0.002	8.5e-04	1.4e-07
69	LOC105372440	3.028	3.252	3.667	2.0e-05	3.6e-06	1.3e-07	3.2e-04	1.2e-04	3.2e-06
70	ROCK1P1	2.491	1.522	2.356	3.2e-10	1.6e-04	1.7e-09	2.6e-08	0.002	7.1e-08
71	LOC728485	1.26	1.44	1.484	2.5e-09	6.2e-12	1.0e-12	1.6e-07	1.2e-09	7.5e-11
72	NAPA-AS1	3.621	4.591	3.81	3.3e-04	3.6e-06	1.3e-04	0.003	1.2e-04	0.001
73	ADGRE4P	2.481	3.189	3.587	0.001	2.4e-05	1.6e-06	0.009	5.4e-04	3.0e-05
74	INTS4P2	4.105	4.004	3.689	3.2e-04	4.3e-04	0.001	0.003	0.005	0.007
75	IQCA1L	4.049	4.679	6.498	4.9e-04	4.0e-05	6.2e-09	0.004	7.8e-04	2.3e-07

We performed Gene Set Enrichment Analysis (GSEA) for the three TDP1-KO cell clones using two the most popular databases Reactome [28] and KEGG [29]. Total GSEA results revealed different pathways associated with DEGs for two databases. We found that the DEGs of TDP1-KO versus WT cells (Table S1) were present for two of them (C6 and F7). There were no significant GSEA results (with p-value < 0.001, adjusted p < 0.01) for the G6 cell clone with the lowest amount of DEGs among the three TDP1-KO cell clones. Several DEGs for sample C6 were associated with the following terms: Glutathione metabolism (according to KEGG database GSEA), and Gene expression (Transcription), Generic Transcription Pathway, Metabolism (according to Reactome database GSEA) (Figure 3A, Table S1). We revealed that DEGs of F7 cells versus WT cells (Figure 3A) were present in processes associated with NF-kappa B signaling pathway, MAPK signaling pathway, Transcriptional misregulation in cancer (according to KEGG database GSEA), and TNFR2 non-canonical NF-kB pathway (according to Reactome database GSEA) (Figure 3B, Table S1).
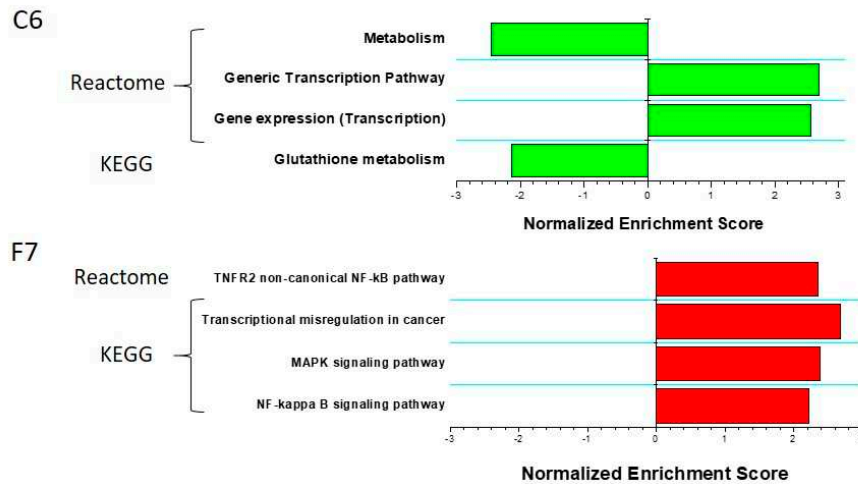
Figure 3. Gene set enrichment analysis (GSEA) of DEGs for comparing HEK293A TDP1-KO cells of the cell clone C6 (A) and F7 (B) versus WT cells. Normalized enrichment scores indicate the distribution of KEGG and Reactome pathways across a list of genes ranked by log2FoldChange. Higher enrichment score indicates a shift of genes belonging to certain pathway towards either end of the ranked list, representing up or down regulation (positive or negative values, respectively).

3. Discussion

DNA repair enzyme TDP1 was initially described and named as an enzyme with phosphodiesterase activity that removes a tyrosyl-containing peptide from a 3'-DNA adducts in DNA single-strand break remaining from TOP1 [30]. It is known that TDP1 hydrolyzes different 3' DNA end blocking lesions including synthetic DNA adducts as a substrate [31]. Other functions of TDP1 in DNA metabolism are also known. This enzyme is able to catalyze the APE1 independent AP site cleavage reaction generating single-strand break with the 3'- and 5'-phosphate termini [7]. Thus TDP1 could be involved in multiple DNA repair pathways. As a member of PLD superfamily, TDP1 is able to catalyze not only hydrolysis but also a transphosphatidylation reaction in the presence of primary alcohols in which they transfer the substrate to the alcohol instead of water [32]. In our previous work we demonstrated [8] that TDP1 is able to undergo a "transphosphooligonucleotidation" reaction, transferring the oligonucleotide substrate residue to the alcohol. This reaction could induce the formation of covalent DNA adducts with different primary alcohol residues, thus regarding TDP1 as not only a repair enzyme but also as a source of DNA damages. Moreover, it is known that TDP1 is located not only in nucleoplasm [33], but also in cytoplasm [34], mitochondria [35], and plasma membrane [36].

In the previous work [37] we made the transcriptomic analysis of the PARP1-knockout HEK293A cells and found much larger changes in the transcriptome of knockout cells versus wild type cells in this case compared with TDP1-KO effect. It was not surprising, since PARP1 is a more widespread enzyme in the cell involved in many processes than TDP1. However, it was interesting to check how TDP1-KO would affect the transcriptome of HEK293A cells, since such studies had not been conducted before. In that work [37] we also examined the effect of 0.1% DMSO and did not find a critical effect of DMSO on the transcription pattern. Differentially expressed genes (DEGs) of the TDP1-KO versus WT cells without DMSO and in the presence of DMSO also were the same. TDP1 is a much less studied protein than PARP1, but it is also involved in many cell processes. We have been investigating this enzyme for the last years, including searching for inhibitors of TDP1 as a potential target for anticancer therapy [3]. Both enzymes TDP1 and PARP1 are considered as participants of the DNA repair. PARP1 recognizes a stalled TOP1cc, catalyzes the PARylation of TDP1 stabilizing TDP1 binding to the DNA proteins [38,39] and recruits other repair proteins to the damage site [40]. In addition to PARylation, TDP1 has been shown to undergo other post-translational modifications

[40]. The list of TDP1 partnership includes TOP1, TDP2, TOP2, APE1, APTX, PNKP, PARP1, APLF, XRCC1, POLB, LIG3 and other proteins [39,41–43]. Previously we have found that PARP1 knockout causes changes in the transcription of several DNA base excision repair (BER) genes [37]. But in this work we did not find any changes in RNA level of repair proteins including all TDP1 partners in TDP1-KO samples. However, TDP1 knockout affected nearly a hundred of DEGs from other cell processes (Tables 1 and 2).

Among the downregulated genes the protein gene SPATA16 (Spermatogenesis Associated 16) had the highest log2FoldChange value (Table 1). The protein SPATA16 localizes to the Golgi apparatus and is involved in spermatogenesis [27]. It is interesting that among the upregulated genes were also found several sperm-specific protein genes and protein genes that are critical in spermatogenesis (Table 2): CFAP58, IZUMO1, and SPANXB1. CFAP58 (Cilia and Flagella Associated Protein 58) is involved in protein localization to motile cilium and sperm axoneme assembly. IZUMO1 (Izumo Sperm-Oocyte Fusion 1) is a sperm-specific protein for sperm-egg plasma membrane binding and fusion. SPANXB1 (SPANX Family Member B1) is a protein involved in regulation of transcription and translation of several testis-specific genes required for spermatogenesis [44]. Spermatogenesis is a composite multi-step process during that male germ cells undergo DNA damages that should be repaired. It was shown [45] that TOP2 removes nucleosomal DNA supercoiling as a part of the normal developmental program of elongating spermatids between steps 9 and 13, and this carries a genetic risk if unresolved double-strand breaks remain. It is known that TDP1 is also able to repair TOP2-induced DNA damage [33,46,47]. It was shown that on these steps of spermatogenesis TOP2 coexists with TDP1 as a DNA repair enzyme known both for TOP1 and TOP2 mediated DNA damages [45,48].

Except participation in protein localization to motile cilium and sperm axoneme assembly during spermatogenesis the protein CFAP58 is also involved in sperm mitochondrial sheath assembly [49]. It is well known that TDP1 protects mitochondrial DNA from lesions and accumulation of TOP1-DNA stuck complex [10]. It was found that TDP1 is the only enzyme in the mitochondria to possess the 3′-hydrolyzing activity on protein–DNA complexes [35], including repairing in mitochondrial genome DNA damages induced by anti-viral and anti-cancer nucleoside analogs which probably enter the mitochondria [50]. The authors of the review [51] note that the mitochondria contain more TDP1 than the nucleus and wrote that the potential that TDP1 could have a greater role in mitochondria than in the nucleus may stem from functions other than DNA repair. Thus our results on the changed expression of CFAP58 and other protein gene SLC25A34 (Table 2) may also indicate the important role of TDP1 in mitochondria. This protein SLC25A34—solute carrier family 25 member 34 belongs to the SLC25 family of mitochondrial carrier proteins expressed in the nervous system [52].

Different groups of scientists consider TDP1 as a critical factor that can contribute to the development of neurological disorders also due to connection such disorders with mitochondrial dysfunction [40,53–55]. Initial evidence that TDP1 deficiency can contribute to the neurological phenotypes was observed for Spinocerebellar Ataxia with Axonal Neuropathy Type 1 (SCAN1). It was identified that a mutation H493R in TDP1 causes accumulation of TOP1cc [5,56], accordingly TDP1-deficient cells are deficient for SSB but not DSB repair [57]. This mutation inhibits the second step of the TDP1 reaction that resolves the TDP1-DNA catalytic intermediate [40], thus SCAN1 cells could accumulate TDP1cc. Different data also are in favor of the fact that TOP1-induced DNA damage could contribute to neurological disorders. For example, it was shown that variants in the TDP1 gene may play a role in Tourette syndrome susceptibility [58]. There are several causes why TDP1 function seen as required in neuronal tissues [53,54]. Neurons are subjected to high level of oxidative attack, due to the high amount of oxygen in the brain relative to other tissues, that causes DNA SSB and DSB that should be repaired. Neurons are terminally differentiated postmitotic cells with the absent DNA replication and has a limited capacity for regeneration. TOP1cc can block transcription, blocked transcription may induce apoptosis [59]. Also apoptosis could be caused due to the accumulation of SSB in the absence of TDP1 with PARP1 high attraction as nick sensor and the depletion of neural NAD+ and ATP [53]. It was shown that TDP1 is required in DNA SSB repair in

primary neural cells and for neural homeostasis because Tdp1 knockout mice were hypersensitive to topotecan, had reduced cerebellar size and hypoalbuminemia, that is feature for SCAN1 patients [57]. In our work we found several DEGs that could be important in neuronal differentiation common for three TDP1-KO HEK293A cell clones (C6, G6, F7, Table 2): TAC1 (Preprotachykinin-1), CHAC1 (ChaC Glutathione Specific Gamma-Glutamylcyclotransferase 1), BEND6 (BEN Domain Containing 6), CACNA1E (Calcium Voltage-Gated Channel Subunit Alpha1 E), DISP3 (Dispatched RND Transporter Family Member 3), TUBB3 (Tubulin Beta 3 Class III). Two of them CHAC1 and BEND6 could be involved in the work of the Notch receptor. Notch receptor is a transmembrane receptor protein working in proliferative signaling during neurogenesis [60]. CACNA1E is involved in a variety of calcium-dependent processes, including neurotransmitter release, gene expression, cell motility, cell division and cell death [61]. TUBB3 may be involved in neurogenesis and axon guidance and maintenance [62].

Another downregulated DEG with high log2FoldChange value is the protein gene DEPP1—DEPP Autophagy Regulator 1 (Table 1). Autophagy is a lysosomal degradation pathway activated under stress conditions including oxidative stress. Neurons strongly depend on this process and the dysfunction of autophagy contributes to the pathologies of neurological disorders [63]. It was shown that DEPP1 induces reactive oxygen species accumulation and mediates the formation of autophagosomes [64] and overexpression of DEPP1 in HEK293 cells induces autophagy [65]. Thus both TDP1 and DEPP1 help cope with oxidative stress.

We analyzed the DEGs using STRING database, version 11.5, to construct a protein–protein interaction (PPI) network for upregulated and downregulated DEGs (Figure 4). We found only four groups of PPI, the remaining DEGs lie separately. Let's look at the DEGs in these groups.
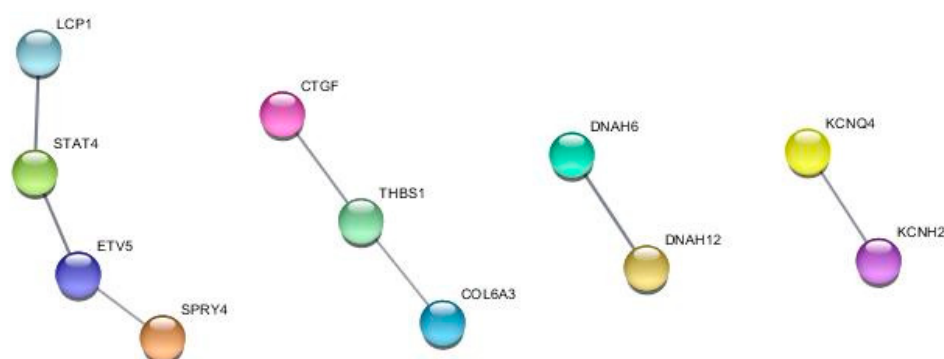

Figure 4. Network of protein-protein interactions of TDP1-dependent genes obtained using the STRING tool. Rendered with Cytoscape v3.7.2. The PPI network was built with a minimum required interaction score 0.7.

It is interesting that in the Human Protein Atlas TDP1 is shown to be located not only in the nucleus, but also the plasma membrane [36]. And besides CACNA1E other protein genes from the first group of the DEGs common for three TDP1-KO HEK293A cell clones were found that are important for cell communication (Table 2).

The proteins of the group of DEGs CTGF(CCN2)-THBS1-COL6A3 (Figure 4) are involved in cell communication and adhesion. CTGF (CCN2, Table 2, Cellular Communication Network Factor 2) is related to platelet-derived growth factor, works in chondrocyte proliferation and differentiation, and cell adhesion in different cell types [66,67]. THBS1 (Thrombospondin 1) is an adhesive glycoprotein that mediates cell-to-cell interactions [68]. COL6A3 (Collagen alpha-3(VI) chain) aids in microfibril formation. It has been shown to bind extracellular matrix proteins and was found in most connective tissues [69].

We performed a Scratch Assay to check the difference in wound healing of TDP1-KO cell clones (C6, G6, F7) vs WT HEK293A cells (Figure 5, and additional video files). We found that there is a

difference of TDP1-KO cells in the value of %Closure/Plate maximum start wound. Thus Tdp1 gene knockout really affects cellular contacts.
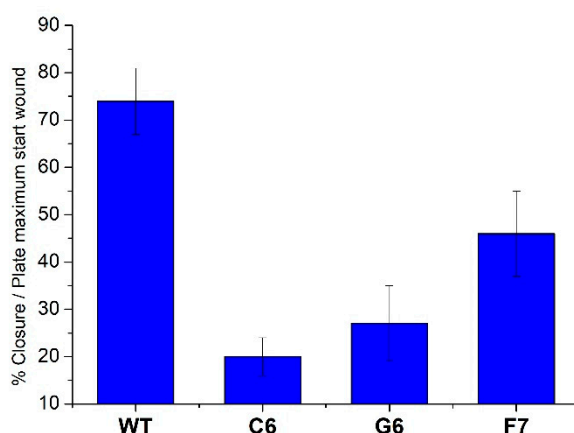

Figure 5. Histogram of wound closure for HEK293A WT and TDP1-KO (C6, G6, F7).

Another group of the membrane protein genes is KCNH2-KCNQ4 (Figure 4) that belong to potassium voltage-gated channel subfamily. KCNH2 (Potassium Voltage-Gated Channel Subfamily H) is a component of a voltage-activated potassium channel found as contributing to the electrical activity of the heart in cardiac muscle, and also in nerve cells, and microglia [70]. KCNQ4 (Potassium voltage-gated channel subfamily KQT member 4) forms a potassium channel that is critical in the regulation of neuronal excitability, especially in sensory cells of the cochlea [71].

The next group (Figure 4) contains DNAH6 (Dynein Axonemal Heavy Chain 6) and DNAH12 (Dynein Axonemal Heavy Chain 12) that belong to axonemal group of a dynein family of cytoskeletal motor proteins. Axonemal dynein work in the axonemes of cilia and flagella and was found in cells that have those structures [72]. Thus this fact can be considered as further evidence that TDP1 is implicated in spermatogenesis.

The fourth group is LCP1-STAT4-ETV5- SPRY4. LCP1 (Lymphocyte Cytosolic Protein 1) is an actin-binding protein initially identified in hematopoietic cells [73] that was identified in two isoforms (L, expressed in hemopoietic cells, and T, found in normal cells of solid tissues). L-plastin has been found in many types of malignant human cells of non-hemopoietic origin suggesting that its expression is induced accompanying tumorigenesis in solid tissues. LCP1 plays a critical role in numerous nonhematopoietic malignancies, thus it was recognized as a tumor biomarker [74]. Among a signaling pathways associated with LCP1 are Interleukin-12 family signaling and Cytokine Signaling in Immune system [49]. Also LCP1 considered as a biomarker for nonalcoholic fatty liver disease [75]. STAT4 (Signal transducer and activator of transcription 4) is a transcription factor belonging to the STAT protein family that is expressed in immune cells and testis [76]. In response to cytokines and growth factors, STAT family members are phosphorylated by the receptor associated kinases, and then form homo- or heterodimers that translocate to the cell nucleus where they act as transcription activators [49]. ETV5 (ETS Variant Transcription Factor 5) enables DNA-binding transcription activator activity, RNA polymerase II-specific and RNA polymerase II transcription regulatory region sequence-specific DNA binding activity. This protein is involved in cellular response to oxidative stress. It is generated in Sertoli cells, and play a crucial role in spermatogenesis [77]. ETV5 overexpression enhanced Th1/Th17 immune response through upregulating the phosphorylation of STAT3 and STAT4 [78]. ETV5 overexpression significantly increased the protein levels of p-STAT3 and p-STAT4. However, upregulation of ETV5 had no significant effect on mRNA levels of STAT3 and STAT4 [78]. SPRY4 (Sprouty RTK Signaling Antagonist 4) is a biomarker gene for transcriptional MAPK Pathway Activity Score (MPAS)—a tool for predicting the sensitivity of

tumor cells to MAPK inhibitors [79]. When using HepG2/C3A cells-based spheroids to model non-alcoholic fatty liver disease was shown increased TGF-β1 signalling through the Ras/RAF/MEK/ERK pathway (prevention or induction of apoptosis or cell cycle progression) including 1.7-fold increase in SPRY4 and the development of a mesenchymal-like phenotype of hepatocytes [80]. ETV5 and SPRY4 were up-regulated under the influence of a Fibroblast growth factor 4 (FGF4), but their expression levels did not change upon cell cycle arrest [81]. In another study, ETV5 and SPRY4 were down-regulated together by the MEK inhibitor [82]. The KEGG database also identified the MAPK pathway as associated with DEG, but only for clone F7 (Figure 3).

4. Materials and Methods

4.1. Tdp1 Knockout HEK293A cells generation

Tdp1 Knockout cell clones (TDP1-KO) were obtained using cell line HEK293A WT (Thermo Fisher Scientific, Waltham, MA, USA) with the CRISPR/Cas9 method [26]. Briefly cell clones with deletions in the region of constitutive proteins encoding exons (Suppl. Figure S1A) were obtained by co-transfection with the plasmids pX458-TDP1-gRNA1 and pX458-TDP1-gRNA2 using a Lipofectamine 3000 Reagent (Thermo Fisher Scientific, Waltham, MA, USA), next the GFP-positive cell population was cell sorted and plated one cell per well onto a 96-well plate. Single-cell clones were analyzed on deletions in Tdp1 gene. Three HEK293A cell clones were found, which contained only alleles with deletions (C6 Δ196bp/Δ197, G6 Δ197bp/Δ197bp, and F7 Δ198bp/Δ196bp). The homozygous deletion was confirmed by PCR, Sanger sequencing [26], and western blotting (Figure S1).

For western blotting, the whole cell extracts (HEK293A WT and clone C6, G6, F7) were separated by Laemmli electrophoresis in 10% SDS-PAAG and transferred on a nitrocellulose membrane (TransBlot Turbo, BIO-RAD, Hercules, CA, USA) by the semidry western blotting technique. It was probed with rabbit antibody to TDP1 (Thermo Fisher Scientific, PA5-27111, Waltham, MA, USA) or rabbit antibody to β-actin (Abcam 8226-100, Cambridge, UK). Then blots were probed with horseradish peroxidase-coupled goat anti-rabbit antibody (1:15,000, made by L. Matveev, Biotechnological Laboratory, ICBFM SB RAS, Novosibirsk, Russia), and immunoreactivity was detected by chemiluminescence (Pierce ECL Western Blotting Substrate, Thermo Scientific, Waltham, MA, USA). The western blotting analysis showed the absence of TDP1 in the TDP1-knockout (TDP1-KO) cells (clones C6, G6, F7 on Figure S1).

4.2. Cell Culture Cytotoxicity Assay

Cytotoxicity of the compounds was examined against human cell lines HEK293A (human embryonic kidney) WT and TDP1-deficient (TDP1-KO, cell clones C6, G6, and F7) on xCELLigence RealTime Cell Analyzer (Agilent, Santa Clara, CA, USA) with RTCA software (Agilent, Santa Clara, CA, USA). The cells were grown in DMEM/F12 medium (Thermo Fisher Scientific, Waltham, MA, USA), with 1× GlutaMAX (Thermo Fisher Scientific, Waltham, MA, USA), 50 IU/mL penicillin, and 50 μg/mL streptomycin (Thermo Fisher Scientific, Waltham, MA, USA), in the presence of 10% FBS (Biolot, Saint-Petersburg, Russia) in 5% CO_2. After formation of a 50–70% layer, topotecan was added to the medium in the indicated concentration, and the cell culture was monitored for several days. The measurements were carried out in two parallel experiments.

4.3. Total RNA Preparation and Transcriptome Sequencing

HEK293A WT and TDP1-KO cells were grown 1-2 million per well in a six-well plate for 20-21 hours to double the number of cells in the well, four replicates for each sample. The RNA samples for the gene expression studies were prepared for four cell lines: 1) WT; and three TDP1-KO cell clones 2) C6; 3) G6; 4) F7. Total RNA was isolated from cells by Trizol and PureLink RNA Mini Kit (Invitrogen, USA) and on-column DNAse I Digestion Set (Sigma-Aldrich, USA). Isolated RNA was measured on Nanodrop 1000 spectrophotometer (Thermo Scientific, USA), and the quality was

estimated by means of measuring RNA Integrity Number (RIN) on Agilent Bioanalyzer 2100 with Agilent RNA 6000 Pico Kit (Agilent, USA).

To isolate poly(A)+ RNA from total RNA by NEBNext Poly(A) mRNA Magnetic Isolation Module (NEB, USA) was performed in SB RAS Genomics Core Facility (ICBFM SB RAS, Novosibirsk, Russia). The quality of enriched poly(A)+ RNA was assessed on Agilent Bioanalyzer 2100 using Agilent RNA 6000 Pico Kit (Agilent, USA). Library was prepared from poly(A)+ RNA by MGIEasy RNA Directional Library Prep Set (MGI Tech Co., Ltd., China). DNA libraries were sequenced with DNBSEQ-G400RS High-throughput Sequencing Set (FCL PE 100) with 30 million coverage per sample on MGIseq 2000 (MGI Tech Co., Ltd., China).

4.4. Bioinformatic Analysis

The obtained reads were aligned to the human genome (hg38, ensembl v38.93) using STAR-2.7.8 [83]. Quality control of the reads was performed using FastQC [84], the "infer_experiment.py" module of RSeQC [85], and the "CollectRnaSeqMetrics" module from Picard [86]. All results were consolidated into a comprehensive report using the MultiQC package [87]. Read quantification was carried out using STAR with the "quantMode GeneCounts" option. Downstream analysis of expression matrix has been performed in DESeq2 package [88]. Subsequently, low-expression genes (sum of reads across all samples less than 10) were filtered from the resulting expression matrix. Vst normalization was applied to the expression matrix to facilitate downstream analysis, including principal component analysis (PCA). Differentially expressed genes were identified using the Wald test, considering genes with a p-value less than 0.01 after adjusting for multiple comparisons. The EnchancedVolcano package [89] was used for visualization of the results. To gain insights into the biological context of the differentially expressed genes, signaling pathway enrichment analysis was performed using the fgsea package [90] with reference to the KEGG database.

4.5. Wound healing assay

Wound healing assay was performed by real time cell imaging on the Cell-IQ instrument in Cell technology facility of the Institute of Cytology and Genetics SB RAS, supported by the budget project FWNR-2022-0015, for HEK293A WT and TDP1-KO cells (C6, G6, F7 cell clones). For the imaging 5*10^5 cells were plated onto a well of 12-well plate. 24 h after plating the cell monolayer was scratched using sterile lancet. The medium was changed to DMEM/F12 (Thermo Fisher Scientific, Waltham, MA, USA) supplemented with 0.2 mM glutamine and 100 U/ml penicillin/streptomicin (Thermofisher Scientific, Waltham, MA, USA). Real time cell imaging was performed in about twenty-four hours using Cell-IQ automated cell culture and analysis system (CM Technologies Oy). Data were processed using Cell-IQ and Origin software.

5. Conclusions

In this work, we performed a transcriptomic analysis of the HEK293A cells with a knockout of the TDP1 gene (TDP1-KO), which encodes the DNA repair enzyme of the same name. We found 15 downregulated and 86 upregulated differentially expressed genes (DEGs) common to the three TDP1-KO biological replicates. Among these DEGs there were no DNA repair enzymes or factors. Apart from its involvement in the removal of various 3'-end adducts from DNA, information about the functions of TDP1 is rather limited. Our findings add some detail to the involvement of TDP1 in mitochondrial function and in the development of some neurodegenerative diseases. We also identified a possible connection between TDP1 and the processes of cell adhesion and communication, spermatogenesis, cytokine response, and MAPK pathway signaling.

Supplementary Materials: The following supporting information can be downloaded at the website of this paper posted on Preprints.org. Figure S1: Scheme of deletion in Tdp1 gene (A); (B) Western-blot analysis of CRISPR/Cas9-induced deletion (B). Figure S2. Principal component analysis (PCA) plot illustrates the transcriptional pattern of cells by the profiles of gene expression in wild type and TDP1 knockout cells. Figure S3. TDP1 knockout effect on HEK293A cells. Volcano Plot for differential gene expression in HEK293A cells with

CRISPR/Cas9-mediated delition in Tdp1 gene (cell clones C6, G6, F7) vs wild type HEK293A cells. Figure S4. Upset barplot of the differentially expressed genes in TDP1-deficient cells compared to the control WT HEK293A cell line. Table S1. TDP1 knockout effect on gene expression in HEK293A cells. Gene set enrichment analysis (GSEA total) results: pathways significantly associated with differentially expressed genes.

References

1. Davies D.R., Interthal H., Champoux J.J., Hol W.G. The crystal structure of human tyrosyl-DNA phosphodiesterase, Tdp1. Structure. 2002, 10, 237-48. https://doi.org/10.1016/s0969-2126(02)00707-4.

2. Yang S.W., Burgin Jr. A.B., Huizenga B.N., Robertson C.A., Yao K.C., Nash H.A. A eukaryotic enzyme that can disjoin dead-end covalentcomplexes between DNA and type I topoisomerases. Proc. Natl Acad. Sci. USA. 1996, 93, 11534–11539. https://doi.org/10.1073/pnas.93.21.11534

3. Zakharenko A.L., Luzina O.A., Chepanova A.A., Dyrkheeva N.S., Salakhutdinov N.F., Lavrik O.I. Natural Products and Their Derivatives as Inhibitors of the DNA Repair Enzyme Tyrosyl-DNA Phosphodiesterase 1. Int J Mol Sci. 2023, 24:5781. https://doi.org/10.3390/ijms24065781.

4. Roca J. The mechanisms of DNA topoisomerases. Trends Biochem Sci. 1995, 20, 156-160. https://doi.org/10.1016/s0968-0004(00)88993-8.

5. Takashima H., Boerkoel C.F., John J., Saifi G.M., Salih M.A., Armstrong D., Mao Y., Quiocho F.A., Roa B.B., Nakagawa M., Stockton D.W., Lupski J.R. Mutation of TDP1, encoding a topoisomerase I-dependent DNA damage repair enzyme, in spinocerebellar ataxia with axonal neuropathy. Nat Genet. 2002, 32, 267–272. https://doi.org/10.1038/ng987.

6. Comeaux E.Q., van Waardenburg R.C. Tyrosyl-DNA phosphodiesterase I resolves both naturally and chemically induced DNA adducts and its potential as a therapeutic target. Drug Metab Rev. 2014, 46, 494-507. https://doi.org/10.3109/03602532.2014.971957.

7. Lebedeva N.A., Rechkunova N.I., El-Khamisy S.F., Lavrik O.I. Tyrosyl-DNA phosphodiesterase 1 initiates repair of apurinic/apyrimidinic sites. Biochimie. 2012, 94, 1749-1753. https://doi.org/10.1016/j.biochi.2012.04.004.

8. Dyrkheeva N., Anarbaev R., Lebedeva N., Kuprushkin M., Kuznetsova A., Kuznetsov N., Rechkunova N., Lavrik O. Human Tyrosyl-DNA phosphodiesterase 1 possesses transphosphooligonucleotidation activity with primary alcohols. Front Cell Dev Biol. 2020, 23;8:604732. https://doi.org/10.3389/fcell.2020.604732.

9. Li J., Summerlin M., Nitiss K.C., Nitiss J.L., Hanakahi L.A. TDP1 is required for efficient non-homologous end joining in human cells. DNA Repair (Amst). 2017, 60, 40-49. https://doi.org/10.1016/j.dnarep.2017.10.003.

10. Chiang S.C., Meagher M., Kassouf N., Hafezparast M., McKinnon P.J., Haywood R., El-Khamisy S.F. Mitochondrial protein-linked DNA breaks perturb mitochondrial gene transcription and trigger free radical-induced DNA damage. Sci Adv. 2017, 28;3(4):e1602506. https://doi.org/10.1126/sciadv.1602506.

11. Chowdhuri S.P., Das B.B. Top1-PARP1 association and beyond: from DNA topology to break repair. NAR Cancer. 2021, 3(1):zcab003. https://doi.org/10.1093/narcan/zcab003.

12. Das B.B., Antony S., Gupta S., Dexheimer T.S., Redon C.E., Garfield S., Shiloh Y., Pommier Y. Optimal function of the DNA repair enzyme TDP1 requires its phosphorylation by ATM and/or DNA-PK. EMBO J. 2009, 28, 3667-3680. https://doi.org/10.1038/emboj.2009.302.

13. Chiang S.C., Carroll J., El-Khamisy S.F. TDP1 serine 81 promotes interaction with DNA ligase IIIalpha and facilitates cell survival following DNA damage. Cell Cycle. 2010, 9, 588-595. https://doi.org/10.4161/cc.9.3.10598.

14. Hudson J.J., Chiang S.C., Wells O.S., Rookyard C., El-Khamisy S.F. SUMO modification of the neuroprotective protein TDP1 facilitates chromosomal single-strand break repair. Nat Commun. 2012, 13;3:733. https://doi.org/10.1038/ncomms1739.

15. Das B.B, Ghosh A., Bhattacharjee S., Bhattacharyya A. Trapped topoisomerase-DNA covalent complexes in the mitochondria and their role in human diseases. Mitochondrion. 2021, 60, 234-244. https://doi.org/10.1016/j.mito.2021.08.017.

16. El-Khamisy S.F., Caldecott K.W. TDP1-dependent DNA single-strand break repair and neurodegeneration. Mutagenesis. 2006, 21, 219-224. https://doi.org/10.1093/mutage/gel024.

17. Zakharenko A., Dyrkheeva N., Lavrik O. Dual DNA topoisomerase 1 and tyrosyl-DNA phosphodiesterase 1 inhibition for improved anticancer activity. Med Res Rev. 2019, 39, 1427-1441. https://doi.org/10.1002/med.21587.

18. Dexheimer T.S., Antony S., Marchand C., Pommier Y. Tyrosyl-DNA phosphodiesterase as a target for anticancer therapy. Anticancer Agents Med Chem. 2008, 8, 381-389. https://doi.org/10.2174/187152008784220357.

19. Meisenberg C., Gilbert D.C., Chalmers A., Haley V., Gollins S., Ward S.E., El-Khamisy S.F. Clinical and cellular roles for TDP1 and TOP1 in modulating colorectal cancer response to irinotecan. Mol Cancer Ther. 2015, 14, 575-585. https://doi.org/10.1158/1535-7163.MCT-14-0762.

20. Liu C., Zhou S., Begum S., Sidransky D., Westra W.H., Brock M., Califano J.A. Increased expression and activity of repair genes TDP1 and XPF in non-small cell lung cancer. Lung Cancer. 2007, 55, 303-311. https://doi.org/10.1016/j.lungcan.2006.10.019.

21. Fam H.K., Walton C., Mitra S.A., Chowdhury M., Osborne N., Choi K., Sun G., Wong P.C., O'Sullivan M.J., Turashvili G., Aparicio S., Triche T.J., Bond M., Pallen C.J., Boerkoel C.F. TDP1 and PARP1 deficiency are cytotoxic to rhabdomyosarcoma cells. Mol Cancer Res. 2013, 11, 1179-1192. https://doi.org/10.1158/1541-7786.MCR-12-0575.

22. Gao R., Das B.B., Chatterjee R., Abaan O.D., Agama K., Matuo R., Vinson C., Meltzer P.S., Pommier Y. Epigenetic and genetic inactivation of tyrosyl-DNA-phosphodiesterase 1 (TDP1) in human lung cancer cells from the NCI-60 panel. DNA Repair (Amst). 2014, 13, 1-9. https://doi.org/10.1016/j.dnarep.2013.09.001.

23. Alagoz M., Gilbert D.C., El-Khamisy S., Chalmers A.J. DNA repair and resistance to topoisomerase I inhibitors: mechanisms, biomarkers and therapeutic targets. Curr Med Chem. 2012, 19, 3874-3885. https://doi.org/10.2174/092986712802002590.

24. Brettrager E.J., van Waardenburg R.C.A.M. Targeting Tyrosyl-DNA phosphodiesterase I to enhance toxicity of phosphodiester linked DNA-adducts. Cancer Drug Resist. 2019, 2, 1153-1163. https://doi.org/10.20517/cdr.2019.91.

25. Leung E., Patel J., Hollywood J.A., Zafar A., Tomek P., Barker D., Pilkington L.I., van Rensburg M., Langley R.J., Helsby N.A., Squire C.J., Baguley B.C., Denny W.A., Reynisson J., Leung I.K.H. Validating TDP1 as an Inhibition Target for the Development of Chemosensitizers for Camptothecin-Based Chemotherapy Drugs. Oncol Ther. 2021, 9, 541-556. https://doi.org/10.1007/s40487-021-00158-0.

26. Dyrkheeva N.S., Filimonov A.S., Luzina O.A., Zakharenko A.L., Ilina E.S., Malakhova A.A., Medvedev S.P., Reynisson J., Volcho K.P., Zakian S.M., Salakhutdinov N.F., Lavrik O.I. New Hybrid Compounds Combining Fragments of Usnic Acid and Monoterpenoids for Effective Tyrosyl-DNA Phosphodiesterase 1 Inhibition. Biomolecules. 2021, 11(7):973. https://doi.org/10.3390/biom11070973.

27. Xu M., Xiao J., Chen J., Li J., Yin L., Zhu H., Zhou Z., Sha J. Identification and characterization of a novel human testis-specific Golgi protein, NYD-SP12. Mol Hum Reprod. 2003, 9, 9-17. https://doi.org/10.1093/molehr/gag005.

28. Griss J., Viteri G., Sidiropoulos K., Nguyen V., Fabregat A., Hermjakob H. ReactomeGSA—Efficient Multi-Omics Comparative Pathway Analysis. Mol Cell Proteomics. 2020, 19, 2115-2125. https://doi.org/10.1074/mcp.TIR120.002155.

29. Kanehisa M. Toward understanding the origin and evolution of cellular organisms. Protein Sci. 2019, 28, 1947-1951. https://doi.org/10.1002/pro.3715.

30. Sun Y., Saha S., Wang W., Saha L.K., Huang S.N., Pommier Y. Excision repair of topoisomerase DNA-protein crosslinks (TOP-DPC). DNA Repair (Amst). 2020, 89:102837. https://doi.org/10.1016/j.dnarep.2020.102837.

31. Dexheimer T.S., Stephen A.G., Fivash M.J., Fisher R.J., Pommier Y. The DNA binding and 3′-end preferential activity of human tyrosyl-DNA phosphodiesterase. Nucleic Acids Res. 2010, 38, 2444-2452. https://doi.org/10.1093/nar/gkp1206.

32. Interthal H., Pouliot J.J., Champoux J.J. The tyrosyl-DNA phosphodiesterase Tdp1 is a member of the phospholipase D superfamily. Proc Natl Acad Sci USA. 2001, 98, 12009-12014. https://doi.org/10.1073/pnas.211429198.

33. Barthelmes H.U., Habermeyer M., Christensen M.O., Mielke C., Interthal H., Pouliot J.J., Boege F., Marko D. TDP1 overexpression in human cells counteracts DNA damage mediated by topoisomerases I and II. J Biol Chem. 2004, 279, 55618-55625. https://doi.org/10.1074/jbc.M405042200.

34. Hirano R., Interthal H., Huang C., Nakamura T., Deguchi K., Choi K., Bhattacharjee M.B., Arimura K., Umehara F., Izumo S., Northrop J.L., Salih M.A., Inoue K., Armstrong D.L., Champoux J.J., Takashima H., Boerkoel C.F. Spinocerebellar ataxia with axonal neuropathy: consequence of a Tdp1 recessive neomorphic mutation? EMBO J. 2007, 26, 4732-4743. https://doi.org/10.1038/sj.emboj.7601885.

35. Das B.B., Dexheimer T.S., Maddali K., Pommier Y.. Role of tyrosyl-DNA phosphodiesterase (TDP1) in mitochondria. Proc Natl Acad Sci USA. 2010, 107, 19790-19795. https://doi.org/10.1073/pnas.1009814107.

36. Sjöstedt E., Zhong W., Fagerberg L., Karlsson M., Mitsios N., Adori C., Oksvold P., Edfors F., Limiszewska A., Hikmet F., Huang J., Du Y., Lin L., Dong Z., Yang L., Liu X., Jiang H., Xu X., Wang J., Yang H., Bolund L, Mardinoglu A., Zhang C., von Feilitzen K., Lindskog C., Pontén F., Luo Y., Hökfelt T., Uhlén M., Mulder J. An atlas of the protein-coding genes in the human, pig, and mouse brain. Science. 2020, 367(6482):eaay5947. https://doi.org/10.1126/science.aay5947.

37. Dyrkheeva N.S., Malakhova A.A., Zakharenko A.L., Okorokova L.S., Shtokalo D.N., Pavlova S.V., Medvedev S.P., Zakian S.M., Nushtaeva A.A., Tupikin A.E., Kabilov M.R., Khodyreva S.N., Luzina O.A., Salakhutdinov N.F., Lavrik O.I. Transcriptomic Analysis of CRISPR/Cas9-Mediated PARP1-Knockout Cells under the Influence of Topotecan and TDP1 Inhibitor. Int J Mol Sci. 2023, 24:5148. https://doi.org/10.3390/ijms24065148.

38. Zhang Y.W., Regairaz M., Seiler J.A., Agama K.K., Doroshow J.H., Pommier Y. Poly(ADP-ribose) polymerase and XPF-ERCC1 participate in distinct pathways for the repair of topoisomerase I-induced DNA damage in mammalian cells. Nucleic Acids Res. 2011, 39, 3607–3620. https://doi.org/10.1093/nar/gkq1304.

39. Das B.B., Huang S.Y., Murai J., Rehman I., Amé J.C., Sengupta S., Das S.K., Majumdar P., Zhang H., Biard D., Majumder H.K., Schreiber V., Pommier Y. PARP1-TDP1 coupling for the repair of topoisomerase I-induced DNA damage. Nucleic Acids Res. 2014, 42, 4435-4449. https://doi.org/10.1093/nar/gku088.

40. Crewe M., Madabhushi R. Topoisomerase-Mediated DNA Damage in Neurological Disorders. Front Aging Neurosci. 2021, 13:751742. https://doi.org/10.3389/fnagi.2021.751742.

41. Szklarczyk D., Kirsch R., Koutrouli M., Nastou K., Mehryary F., Hachilif R., Gable A.L., Fang T., Doncheva N.T., Pyysalo S., Bork P., Jensen L.J., von Mering C. The STRING database in 2023: protein-protein association networks and functional enrichment analyses for any sequenced genome of interest. Nucleic Acids Res. 2023, 51(D1):D638-D646. https://doi.org/10.1093/nar/gkac1000.

42. Moor N.A., Vasil'eva I.A., Anarbaev R.O., Antson A.A., Lavrik O.I. Quantitative characterization of protein-protein complexes involved in base excision DNA repair. Nucleic Acids Res. 2015, 43, 6009-6022. https://doi.org/10.1093/nar/gkv569.

43. Pommier Y., Huang S.N., Gao R., Das B.B., Murai J., Marchand C. Tyrosyl-DNA-phosphodiesterases (TDP1 and TDP2). DNA Repair (Amst). 2014, 19, 114-129. https://doi.org/10.1016/j.dnarep.2014.03.020.

44. Hansen S., Eichler E.E., Fullerton S.M., Carrell D. SPANX gene variation in fertile and infertile males. Syst Biol Reprod Med. 2010, 55, 18-26. https://doi.org/10.3109/19396360903312015.

45. Leduc F., Maquennehan V., Nkoma G.B., Boissonneault G. DNA damage response during chromatin remodeling in elongating spermatids of mice. Biol Reprod. 2008, 78, 324-332. https://doi.org/10.1095/biolreprod.107.064162.

46. Nitiss K.C., Malik M., He X., White S.W., Nitiss J.L. Tyrosyl-DNA phosphodiesterase (Tdp1) participates in the repair of Top2-mediated DNA damage. Proc Natl Acad Sci USA. 2006, 103, 8953-8958. https://doi.org/10.1073/pnas.0603455103.

47. Borda M.A., Palmitelli M., Veron G., González-Cid M., de Campos Nebel M. Tyrosyl-DNA-phosphodiesterase I (TDP1) participates in the removal and repair of stabilized-Top2α cleavage complexes in human cells. Mutat Res. 2015, 781:37-48. https://doi.org/10.1016/j.mrfmmm.2015.09.003.

48. Shaman J.A., Prisztoka R., Ward W.S. Topoisomerase IIB and an extracellular nuclease interact to digest sperm DNA in an apoptotic-like manner. Biol Reprod. 2006, 75, 741-748. https://doi.org/10.1095/biolreprod.106.055178.

49. Stelzer G., Rosen N., Plaschkes I., Zimmerman S., Twik M., Fishilevich S., Stein T.I., Nudel R., Lieder I., Mazor Y., Kaplan S., Dahary D., Warshawsky D., Guan-Golan Y., Kohn A., Rappaport N., Safran M., Lancet D. The GeneCards Suite: From Gene Data Mining to Disease Genome Sequence Analyses. Curr Protoc Bioinformatics. 2016, 54:1.30.1-1.30.33. https://doi.org/10.1002/cpbi.5.

50. Huang S.-Y. N., Pommier Y. Mammalian Tyrosyl-DNA Phosphodiesterases in the Context of Mitochondrial DNA Repair. Int J Mol Sci. 2019, 20:3015. https://doi.org/10.3390/ijms20123015.

51. Sykora P., Wilson D.M. 3rd, Bohr V.A. Repair of persistent strand breaks in the mitochondrial genome. Mech Ageing Dev. 2012, 133, 169-175. https://doi.org/10.1016/j.mad.2011.11.003.

52. Haitina T., Lindblom J., Renström T., Fredriksson R. Fourteen novel human members of mitochondrial solute carrier family 25 (SLC25) widely expressed in the central nervous system. Genomics. 2006, 88, 779-790. https://doi.org/10.1016/j.ygeno.2006.06.016.

53. El-Khamisy S.F. To live or to die: a matter of processing damaged DNA termini in neurons. EMBO Mol Med. 2011, 3, 78–88. https://doi.org/10.1002/emmm.201000114

54. Rass U., Ahel I., West S.C. Defective DNA Repair and Neurodegenerative Disease. Cell. 2007, 130, 991-1004. https://doi.org/10.1016/j.cell.2007.08.043.

55. Van Waardenburg R.C.A.M. Tyrosyl-DNA Phosphodiesterase I a critical survival factor for neuronal development and homeostasis. J Neurol Neuromedicine. 2016, 1, 25-29. https://doi.org/10.29245/2572.942x/2016/5.1048.

56. El-Khamisy S.F., Caldecott K.W. DNA single-strand break repair and spinocerebellar ataxia with axonal neuropathy-1. DNA single-strand break repair and spinocerebellar ataxia with axonal neuropathy-1. Neuroscience. 2007, 145, 1260-1266. https://doi.org/10.1016/j.neuroscience.2006.08.048.

57. Katyal S., El-Khamisy S.F., Russel H.R., Li Y., Ju L., Caldecott K.W., McKinnon P.J. TDP1 facilitates chromosomal single-strand break repair in neurons and is neuroprotective in vivo. EMBO J. 2007, 26, 4720-4731. https://doi.org/10.1038/sj.emboj.7601869.

58. Wu B.-T., Lin W.-Y., Chou I.-C., Liu H.-P., Lee C.-C., Tsai Y., Wu W.-C., Tsai F.-J. Association of Tyrosyl-DNA Phosphodiesterase 1 Polymorphism with Tourette Syndrome in Taiwanese Patients. J Clin Lab Anal. 2013, 27, 323-327. https://doi.org/10.1002/jcla.21606.

59. Ljungman M., Lane D.P. Transcription—guarding the genome by sensing DNA damage. Nat Rev Cancer. 2004, 4, 727-737. https://doi.org/10.1038/nrc1435.

60. Brou C., Logeat F., Gupta N., Bessia C., LeBail O., Doedens J.R., Cumano A., Roux P., Black R.A., Israël A. A novel proteolytic cleavage involved in Notch signaling: the role of the disintegrin-metalloprotease TACE. Mol Cell. 2000, 5, 207-216. https://doi.org/10.1016/s1097-2765(00)80417-7.

61. Soong T.W., Stea A., Hodson C.D., Dubel S.J., Vincent S.R., Snutch T.P. Structure and functional expression of a member of the low voltage-activated calcium channel family. Science. 1993, 260, 1133–1136. https://doi.org/10.1126/science.8388125.

62. Caccamo D.V., Herman M.M., Frankfurter A., Katsetos C.D., Collins V.P., Rubinstein L.J. An immunohistochemical study of neuropeptides and neuronal cytoskeletal proteins in the neuroepithelial component of a spontaneous murine ovarian teratoma. Primitive neuroepithelium displays immunoreactivity for neuropeptides and neuron-associated beta-tubulin isotype. Am J Pathol. 1989, 135, 801-813.

63. Gómez-Virgilio L., Silva-Lucero M.D., Flores-Morelos D.S., Gallardo-Nieto J., Lopez-Toledo G., Abarca-Fernandez A.M., Zacapala-Gómez A.E., Luna-Muñoz J., Montiel-Sosa F., Soto-Rojas L.O., Pacheco-Herrero M., Cardenas-Aguayo M.D. Autophagy: A Key Regulator of Homeostasis and Disease: An Overview of Molecular Mechanisms and Modulators. Cells. 2022, 11(15):2262. https://doi.org/10.3390/cells11152262.

64. Salcher S., Hermann M., Kiechl-Kohlendorfer U., Ausserlechner M.J., Obexer P. C10ORF10/DEPP-mediated ROS accumulation is a critical modulator of FOXO3-induced autophagy. Mol Cancer. 2017 May 25;16(1):95. https://doi.org/10.1186/s12943-017-0661-4.

65. Stepp M.W., Folz R.J., Yu J., Zelko I.N. The c10orf10 gene product is a new link between oxidative stress and autophagy. Biochim Biophys Acta. 2014, 1843, 1076-1088. https://doi.org/10.1016/j.bbamcr.2014.02.003.

66. Jun J.I., Lau L.F. Taking aim at the extracellular matrix: CCN proteins as emerging therapeutic targets. Nat Rev Drug Discov. 2011, 10, 945–963. https://doi.org/10.1038/nrd3599.

67. Hall-Glenn F., Lyons K.M. Roles for CCN2 in normal physiological processes. Cell Mol Life Sci. 2011, 68, 3209–3217. https://doi.org/10.1007/s00018-011-0782-7.

68. Kaur S., Roberts D.D. Why do humans need thrombospondin-1? J Cell Commun Signal. 2023, 17, 485-493. https://doi.org/10.1007/s12079-023-00722-5.

69. Lamandé S.R., Mörgelin M., Adams N.E., Selan C., Allen J.M. The C5 domain of the collagen VI alpha3(VI) chain is critical for extracellular microfibril formation and is present in the extracellular matrix of cultured cells. The Journal of Biological Chemistry. 2006, 281, 16607–16614. https://doi.org/10.1074/jbc.M510192200.

70. Warmke J.W., Ganetsky B.A family of potassium channel genes related to eag in Drosophila and mammals. Proc Natl Acad Sci USA. 1994, 91, 3438-3442.. https://doi.org/10.1073/pnas.91.8.3438.

71. Kubisch C., Schroeder B.C., Friedrich T., Lutjohann B., El-Amraoui A., Marlin S., Petit C., Jentsch T.J. KCNQ4, a novel potassium channel expressed in sensory outer hair cells, is mutated in dominant deafness. Cell. 1999, 96, 437–446. https://doi.org/10.1016/S0092-8674(00)80556-5.

72. Hu F., Xu K., Zhou Y., Wu C., Wang S., Xiao J., Wen M., Zhao R., Luo K., Tao M., Duan W., Liu S. Different expression patterns of sperm motility-related genes in testis of diploid and tetraploid cyprinid fish. Biol Reprod. 2017, 96, 907-920. https://doi.org/10.1093/biolre/iox010.

73. Lin C.S., Park T., Chen Z.P., Leavitt J. Human plastin genes. Comparative gene structure, chromosome location, and differential expression in normal and neoplastic cells. J BiolChem. 1993, 268, 2781–2792. https://doi.org/10.1016/S0021-9258(18)53842-4.

74. Chen C., Cai Q., He W., Lam T.B., Lin J., Zhao Y., Chen X., Gu P., Huang H., Xue M., Liu H. AP4 modulated by the PI3K/AKT pathway promotes prostate cancer proliferation and metastasis of prostate cancer via upregulating L-plastin. Cell Death Dis. 2017, 8, e3060. https://doi.org/10.1038/cddis.2017.437.

75. Miller M.H., Walsh S.V., Atrih A., Huang J. T.-J., Ferguson M.A. J., Dillon J.F. Serum proteome of nonalcoholic fatty liver disease: a multimodal approach to discovery of biomarkers of nonalcoholic steatohepatitis. J Gastroenterol Hepatol. 2014, 29, 1839-1847. https://doi.org/10.1111/jgh.12614.

76. O'Shea J.J., Lahesmaa L., Vahedi G., Laurence A., Kanno Y. Genomic views of STAT function in CD4+ T helper cell differentiation: new technology brings new insights and new questions. Nat Rev Immunol. 2011, 11, 239–250. https://doi.org/10.1038/nri2958.

77. Morrow C.M., Hostetler C.E., Griswold M.D., Hofmann M.C., Murphy K.M., Cooke P.S., Hess R.A. ETV5 is required for continuous spermatogenesis in adult mice and may mediate blood testes barrier function and testicular immune privilege. Ann NY Acad Sci. 2007,1120, 144-151. https://doi.org/10.1196/annals.1411.005.

78. Shi Y., Dai S., Qiu C., Wang T., Zhou Y., Xue C., Yao J., Xu Y. MicroRNA-219a-5p suppress-es intestinal inflammation through inhibiting Th1/Th17-mediated immune responses in inflammatory bowel disease. Mucosal Immunol. 2020, 13, 303-312. https://doi.org/10.1038/s41385-019-0216-7.

79. Wagle M.C., Kirouac D., Klijn C., Liu B., Mahajan S., Junttila M., Moffat J., Merchant M., Huw L., Wongchenko M., Okrah K., Srinivasan S., Mounir Z., Sumiyoshi T., Haverty P.M., Yauch R.L., Yan Y., Kabbarah O., Hampton G., Amler L., Ramanujan S., Lackner M.R., Huang S.A. A transcriptional MAPK Pathway Activity Score (MPAS) is a clinically relevant biomarker in multiple cancer types. NPJ Precis Oncol. 2018, 2(1):7. https://doi.org/10.1038/s41698-018-0051-4.

80. Frandsen H.S., Vej-Nielsen J.M., Smith L.E., Sun L., Mikkelsen K.L., Thulesen A.P., Hagensen C.E., Yang F., Rogowska-Wrzesinska A. Mapping Proteome and Lipidome Changes in Early-Onset Non-Alcoholic Fatty Liver Disease Using Hepatic 3D Spheroids. Cells. 2022, 11, 3216. https://doi.org/10.3390/cells11203216.

81. Chesnokov M.S., Yadav A., Chefetz. I. Optimized transcriptional signature for evaluation of MEK/ERK pathway baseline activity and long-term modulations in ovarian cancer. Int. J. Mol. Sci. 2022, 23, 13365. https://doi.org/10.3390/ijms232113365.

82. Martin-Vega A., Earnest S., Augustyn A., Wichaidit C., Gazdar A., Girard L., Peyton M., Kollipara R.K., Minna J.D., Johnson J.E., Cobb M.H. ASCL1-ERK1/2 Axis: ASCL1 restrains ERK1/2 via the dual specificity phosphatase DUSP6 to promote survival of a subset of neuroendocrine lung cancers. bioRxiv. 2023 Jun 15:2023.06.15.545148. https://doi.org/10.1101/2023.06.15.545148.

83. Dobin A., Davis C.A., Schlesinger F., Drenkow J., Zaleski C., Jha S., Batut P., Chaisson M., Gingeras T.R. STAR: ultrafast universal RNA-seq aligner. Bioinformatics. 2013, 29, 15-21. https://doi.org/10.1093/bioinformatics/bts635.

84. Andrews S. FastQC: a quality control tool for high throughput sequence data. 2010. Available online at: http://www.bioinformatics.babraham.ac.uk/projects/fastqc.

85.   Wang L., Wang S., Li W. RSeQC: quality control of RNA-seq experiments. Bioinformatics (Oxford, England), 2012, 28, 2184–2185. https://doi.org/10.1093/bioinformatics/bts356.

86.   "Picard Toolkit." 2019. Broad Institute, GitHub Repository. https://broadinstitute.github.io/picard/; Broad Institute

87.   Ewels P., Magnusson M., Lundin S., Käller M. MultiQC: Summarize analysis results for multiple tools and samples in a single report. Bioinformatics. 2016 Oct 1;32(19):3047-8. https://doi.org/10.1093/bioinformatics/btw354.

88.   Love M.I., Huber W., Anders S. Moderated estimation of fold change and dispersion for RNA-seq data with DESeq2. Genome Biology. 2014, 15, 550. https://doi.org/10.1186/s13059-014-0550-8.

89.   Blighe K., Rana S., Lewis M. EnhancedVolcano: Publication-ready volcano plots with enhanced colouring and labeling. 2023. R package version 1.18.0. https://github.com/kevinblighe/EnhancedVolcano.

90.   Korotkevich G., Sukhov V., Sergushichev A. Fast gene set enrichment analysis. bioRxiv. 2019. https://doi.org/10.1101/060012.